EFFICIENT SMOOTHING AND INTERPOLATION OF VELOCITY MODELS FOR SEISMIC WAVEFRONT CONSTRUCTION ALGORITHMS

A Thesis

by

BO CHEN

Submitted to the Office of Graduate Studies of
Texas A&M University
in partial fulfillment of the requirements for the degree of

MASTER OF SCIENCE

August 2011

Major Subject: Geophysics

EFFICIENT SMOOTHING AND INTERPOLATION OF VELOCITY MODELS FOR SEISMIC WAVEFRONT CONSTRUCTION ALGORITHMS

A Thesis

by

BO CHEN

Submitted to the Office of Graduate Studies of
Texas A&M University
in partial fulfillment of the requirements for the degree of

MASTER OF SCIENCE

Approved by:

Chair of Committee,	Richard L. Gibson, Jr.
Committee Members,	Mark E. Everett
	Nancy M. Amato
Head of Department,	Andreas Kronenberg

August 2011

Major Subject: Geophysics

ABSTRACT

Efficient Smoothing and Interpolation of Velocity Models
for Seismic Wavefront Construction Algorithms. (August 2011)
Bo Chen, B.S., Wuhan University, China;
M.S., Texas A&M University
Chair of Advisory Committee: Dr. Richard L. Gibson, Jr.

The wavefront construction (WFC) method is an effective tool to compute seismic ray fields and has wide applications. This paper applies the WFC method to a heterogeneous earth model represented as a 3-D grid instead of a sequence of smooth layers, as the layered model is insufficient for the regions with complex geological structures. In order to utilize gridded models, highly heterogeneous models must be smoothed for reliable numerical results. A new velocity gradient smoothing method is proposed that is able to control quantitatively the smoothness of the velocity model while preserving the main structural characteristics of the original model. A modified inverse distance weighting method is applied to obtain velocities or densities at an arbitrary point in the model for successive wavefront propagation. A very complex 3-D grid model based on the standard Marmousi reference model is tested to compare the new approach to alternative smoothing schemes, and the first arrival traveltimes from the WFC method are compared with results from an eikonal solver. These results are obtained more quickly, but the algorithm is restricted to computing only first arrivals. However, comparison helps to establish the accuracy of the WFC solutions and assess the influence of the smoothing schemes. The modeling comparisons verify the effectiveness of the proposed smoothing methods and the enhanced performance of the WFC algorithm with the 3-D grid model.

To my supportive family

ACKNOWLEDGMENTS

I thank my parents for their constant support and care. I thank the group members in the Theoretical Geophysics Lab, Au Kim Vuong, Dehan Zhu, Jianchao Ge, John Priest, Kai Gao, Rituparna Basu, Zhonghai Liu, and Tarun Jain from Department of Computer Engineering & Science. It was nice to discuss the research topics with you and share the meaningful moments in the lab.

I deeply appreciate Dr. Gibson's help and directions. He not only helped me on the research project but also helped me to form the conscientious and careful habit and the curiosity for studying. I also appreciate my committee members, Dr. Everett and Dr. Amato. They gave me great advice on how to study and how to be a continuously-improving researcher like themselves.

TABLE OF CONTENTS

LIST OF FIGURES

FIGURE Page

FIGURE Page

CHAPTER I

INTRODUCTION

The wavefront construction method (WFC) plays an important role in seismic modeling and exploration seismology (Carcione and et al, 2002; Fehler and Huang, 2002; Gjøystdal et al, 2007). WFC has been utilized robustly in isotropic and anisotropic 3-D stratified models (Lai et al, 2009; Gibson et al, 2005; Červený, 2001; Vinje et al, 1993). Wavefronts consisting of rays arranged in a triangular or quadrilateral network are propagated stepwise through the model. Certain parameter quantities that provide estimates of accuracy of the ray solution, such as the traveltime errors, are checked between the rays of each wavefront mesh cell during the wavefield propagation. If such differences are over a preset threshold, new rays will be interpolated in the mesh cell. In this way, the ray field is evenly distributed throughout the model space with controlled accuracy. Receivers record the multivalued traveltimes and amplitudes when the wavefronts pass them.

This project aims to apply the wavefront construction method to a 3-D, heterogeneous earth model. In many algorithms, the earth model is described as a stratified medium with piecewise constant properties, which is the simplest parameterization for ray methods. However, when there are complex 3-D geological structures, such as faults, pinch-outs, salt domes or complex geological formations, the layered model is inadequate to describe the detailed variation of earth properties. In contrast, a 3-D model parameterized using values specified at a regular grid of points includes more specific material property information about the earth. The introduction of a 3-D model to the wavefront construction also simplifies use for migration applications,

---

The thesis follows the style and format of Geophysics.

an important tool in applied seismology, since it uses gridded models in most cases. Therefore, this project aims to apply the wavefront construction method to a 3-D, heterogeneous earth model, to get more accurate travel time, amplitude information of ray paths traveling through the earth and also be compatible with the prevailing migration algorithms.

In order to fulfill this goal, two issues need to be addressed. First of all, the gridded earth model needs to be smoothed for the application of wavefront construction. Second, a fast and accurate interpolation for seismic velocities, their first direvatives and densities is in demand at an arbitrary point in the gridded earth model. Several previous works (Gajewski et al., 2002, Coman and Gajewski, 2001) investigated the feasibility of a 3-D grid model applied to WFC and its advantage over the layered model. However, this previous work has not considered the selection of smoothing and elastic parameter interpolation schemes in detail, which are essential procedures for incorporating 3-D grid models in the WFC method. A running average smoothing scheme and a linear elastic parameter interpolation were applied, but the running average smoothing is not sensitive to the directionally oriented features in the earth model. In addition, it tends to apply the same degree of smoothing over the entire model without considering local parameter variations. As for the linear elastic parameter interpolation, it is a fast solution, but it fails to generate second order continuous interpolating values. Therefore, large and unnecessary differences are potentially introduced to the model by the running average smoothing and linear elastic parameter interpolation schemes (Gajewski et al., 2002, Coman and Gajewski, 2001).

One important issue leading to errors in many cases, is that the ray theory is based on the high frequency approximation, implying that an earth model is relatively smooth. This asymptotic assumption states that the attributes calculated by ray tracing, such as traveltime and amplitude, are generally stable if interface

normals and gradients of elastic parameters (e.g., P- and S-wave velocities for an isotropic medium) vary smoothly within a region surrounding the ray (Gjøystdal et al, 2007). This region depends on the dominant seismic frequency and is referred to as the Fresnel volume (Červený and Soares, 1992), i.e. within a wavelength distance in each space direction. There are several methods proposed to generate sufficiently smooth models from arbitrarily heterogeneous initial models for ray methods, including running average smoothing (Alde et al., 2002), Gaussian smoothing (Pacheco and Larner, 2005), minimizing the Sobolev norm of slowness (Bulant, 2002, Žáček, 2002), and structure-oriented smoothing (Hale, 2009). These methods are able to increase the smoothness visually based on various attributes, such as Gaussian distribution function, Sobolev norm, structure tensor and etc. However, the attributes these smoothing methods utilize are not directly related to the smoothness requirement of ray tracing. Consequently, it is difficult to establish any quantitative criteria for parameterizing these methods to satisfy the smoothness requirements without too much alteration of the earth model. In this paper, we outline a new velocity gradient smoothing method that will satisfy the requirements of ray methods. This new method is able to precisely control the velocity variations of the model while preserving the main structural characteristics of the original model.

Additionally, interpolating velocity and density between grid points is when wave fronts are propagated through the earth model in the simulation. Hence, an interpolation scheme is essential to estimate these physical properties. Because the interpolation is used frequently during wavefront construction, the interpolation of seismic properties must have low computation costs and high accuracy. Several techniques have been developed for the spatial interpolation applications, such as the linear interpolation method (Coman, 2001), cubic spline method (Massopust, 2010), Kriging method and Inverse Distance Weighting method (Kravchenko, 2003). However, these

interpolation methods cause undesirable oscillations at locations where interpolated values change rapidly, an effect sometimes referred to as the bull's eye problem. Furthermore, the implementations of cubic spline and Kriging methods are also more computationally intensive than linear interpolation and the inverse distance weighting method. We utilize an improved inverse distance weighting method (Nielson, 1993) to avoid the bull's eye problem, to better retain the model's variation trend and still be computationally efficient.

This paper investigates the smoothing issues with the goal of applying 3D grid model to WFC and improving its performance in efficiency and accuracy. Below we first review the WFC algorithm and the primary challenges encountered in applying it to grid-based models. We then briefly review the interpolation scheme (Nielson, 1993), which, to the best of our knowledge, has not been applied in the literature for ray tracing approaches or WFC. The new velocity gradient smoothing method is then presented and first demonstrated in application to a relatively simple model with wedge structure. Because the only heterogeneity is at the interface between the wedge and the surrounding homogeneous medium, this model provides a simply example to compare and contrast the behavior of several smoothing methods and to demonstrate the advantages of the new approach. Finally, we apply the smoothing and interpolation schemes using a simple wedge model and a 3-D form of the Marmousi model to provide a more stringent test of the various methods, again showing the advantages in accuracy of the velocity gradient smoothing method.

CHAPTER II

METHOD

2.1. Wavefront Construction

Wavefront construction (WFC) methods, an extension of standard ray tracing integrating kinematic and dynamic ray tracing (Červený and Horn, 1980), have been applied to isotropic and anisotropic media to simulate wave propagation (Červený, 2001; Gajewski and Vanelle, 2002; Gibson et al, 2005; Lai et al, 2009; Lee and Gibson, 2007; Vinje et al, 1993). In the standard two point ray tracing method, all the rays are computed directly from the source (or from the initial surface). Sufficient density of the ray field in the target region is ensured by subdivision of the ray-parameter domain. In the WFC method, the rays are used to compute the wavefronts successively. At each wavefront, the number of rays is adjusted according to the local behavior of the ray field. Consequently, the ray field in the WFC method is always sufficiently dense, and the succeeding interpolations are sufficiently accurate. Moreover, the computed rays are shorter because they are not computed directly from the source but rather from the individual wavefronts. Better robustness and accuracy are thus obtained for the traveltime and amplitude computation in models with complex structures. Its solutions can be applied to generate synthetic seismograms, tomography update, reservoir analysis and etc. Additionally, it can calculate multiple arrivals (Vinje et al, 1996), which are important for further processing procedures and inversion algorithms.

WFC begins by initializing a set of rays near the source (Gibson et al., 2005). Each ray segment is extended at equal temporal increments through the model with smooth variations of elastic parameters. All the rays form a surface with constant

traveltime, i.e. a wavefront, at a certain time. As rays propagate forward and diverge, new rays are interpolated to maintain a certain ray density in the medium and the traveltime calculation accuracy along the ray. Several interpolation criteria have been proposed (Lee and Gibson, 2007; Vinje, 1997), such as the distance and angle between adjacent rays or traveltime variations. In this project, the traveltime perturbation, i.e. the difference between actual traveltimes computed by paraxial ray tracing, is selected as the interpolation criterion, which is a more physically meaningful measure because the traveltime on a certain wavefront is supposed to be the same by definition, and the numerical difference is an error estimate can serve as a threshold for interpolation (Lee and Gibson, 2007). A certain wavefront is computed from the previous wavefront by tracing a succession of short ray elements. Travel time and amplitude are computed along each ray element while the rays propagate. Additional detailes regarding numerical implementations can be found in Appendix A.

2.2. 3-D Gridded Models - Interpolation

Physical properties, such as velocity, density and spatial derivatives of velocity, are required to compute the traveltime, amplitude and ray path (see equations A.1- A.3), key results required in wavefront construction methods (Gibson et al, 2005). As the wavefront meshes are irregularly spaced during propagation, interpolation is indispensable to obtain the property values at the wavefront mesh locations (points on ray paths) based on the properties at the actual grid points included in the earth model. It is important for the interpolation approach to preserve the characteristics of the continuous fields and the quality of the results with high computation speed. Several methods, models and techniques have been developed for the interpolation

procedure, such as the linear interpolation method, cubic spline method, Kriging method and etc. These methods address the interpolation respectively with different assumptions and means. Linear interpolation is easy to implement. However, it can only provide the second order approximation with discontinuous derivatives. Nor is it second-order continuous at the grid points. The cubic spline interpolation can result in strong oscillations when large velocity contrasts are present. Kriging interpolation requires much more computation time and effort compared to other interpolation techniques. Consequently, Kriging does not meet the requirements of the wavefront construction algorithm, which performs interpolation repeatedly for each ray point traveling in space. For these reasons, we instead utilize an improved Inverse Distance Weighting (IDW) method (Nielson 1993) is applied to better reflect the velocity field features and improve the precision. In this approach, the interpolated velocity is inversely proportional to d_i^n, where d_i is the distance from the i'th grid node, and n is an exponent that is usually set to 2. A detailed derivation is presented in Appendix B.

2.3. 3-D Gridded Models - Smoothing

The smoothing requirement of ray methods stems from the high frequency approximation involved in deriving the ray equations, which implies that the material parameters of the medium may not vary greatly over distances on the order of a wavelength λ (Červený, 2001). Several smoothing schemes have been proposed to increase smoothness based on various attributes, such as running average smoothing (Alde et al., 2002), Gaussian smoothing (Pacheco and Larner, 2005), minimizing the Sobolev norm of slowness (Bulant, 2002; Žáček, 2002), and structure-oriented smoothing (Hale, 2009). However, the quantities these smoothing schemes are based upon,

such as Sobolev norm and structure tensor, are not directly related to the smoothness requirement for ray tracing. Therefore, it is difficult to establish any quantitative criteria for the these methods to adapt the model to ray tracing without significantly changing wave propagation behavior in the earth model (Gray, 2000).

To gain insight into the ray method validity conditions, the concept of Fresnel volumes is invoked (Kravtsov and Orlov, 1990). The parameters of the medium and the parameters of the wave under consideration (amplitude and slowness vector) must not vary significantly over the cross section of the Fresnel volume. If we denote the maximum width r_F of the Fresnel volume cross-section perpendicular to the ray direction, we can write

$$r_F \left| \frac{\nabla_\perp v}{v} \right| << 1 \tag{2.1}$$

Here $\nabla_\perp$ denotes the gradient perpendicular to the ray (Kravtsov and Orlov, 1990). We can develop a smoothing equation beginning with this inequality and estimating the perpendicular gradient from values on the velocity model grid. Begin by recalling that the radius of the Fresnel volume r_F is half the wave length $\lambda/2$ (Červený and Soares, 1992). Δv is the velocity difference between two grid points under consideration, and Δd is the distance between two grid points. Since rays potentially can travel in any direction, for the sake of completeness, $\Delta v/\Delta d$ of all the neighboring points around the point of interest are utilized to estimate this perpendicular gradient. v_{avg} is the average propagation velocity at a given point. The inequality then can be rewritten in terms of 3-D grid model parameters as

$$\Delta v \cdot \frac{\lambda}{2\Delta d} << v_{avg} \tag{2.2}$$

As long as this inequality is honored, the applicability condition of the ray method is met. However, sometimes the rule can be relaxed and the ray methods can be

applied to the medium where the velocity difference is not much smaller than the prevailing velocity (Červený, 2001). We performed extensive numerical testing and find that the left hand side of the inequality 2.2 can range from 0 to 25% of the right hand side and give reasonable results. Here 15% is utilized in the test such that the smoothness requirement is met and the model's feathers are retained. To supplement these inequities and formulate a criterion that quantitatively determines the satisfactory smoothing degree, a threshold factor k is introduced to quantify how small the velocity difference is compared to the average velocity. The value k is the ratio between the velocity difference within half the wavelength and average velocity. If $\Delta v \cdot \frac{\lambda}{\Delta d} \leq k \cdot v_{avg}$, the velocity variation is considered small and meet the ray tracing high-frequency assumption. Hence, the smoothing criteria for WFC application can be established as

$$\Delta v \cdot \frac{\lambda}{2\Delta d} < k v_{avg} \tag{2.3}$$

Since the rays can potentially travel through any locations in any directions, every grid point in the earth model is compared with its adjacent points in all directions. Let $v_{i,j,k}$ be the velocity at the considering point P. $v_{i+r,j+s,k+t}$ represents the velocity at a neighboring point of the point of interest P, where $r, s, t \in \{-1, 0, 1\}$.

If

$$\frac{v_{i+r,j+s,k+t} - v_{i,j,k}}{2\Delta d} \cdot \lambda > k' v_{avg} \tag{2.4}$$

velocity $v_{i,j,k}$ and $v_{i+r,j+s,k+t}$ will be adjusted, where

$$\Delta d = \sqrt{(r \times \Delta d_x)^2 + (s \times \Delta d_y)^2 + (t \times \Delta d_z)^2} \tag{2.5}$$

and Δd_x, Δd_y, Δd_z are the grid spacings in the x, y, and z directions. k' is the ratio of one pair adjacent velocity difference within half the wavelength to average velocity. For any specific grid point, its velocity is compared and possibly adjusted multiple

times, so k' should be smaller than k to guarantee that all the neighboring velocity differences are smaller than desired kv_{avg} in the model.

Average velocity is related to wavelength through

$$v_{avg} = \lambda \times f, \tag{2.6}$$

where f is prevailing frequency.

Insert equation (2.6) into (2.4),

$$\frac{v_{i+r,j+s,k+t} - v_{i,j,k}}{\Delta d} \cdot \lambda > k'\lambda f \tag{2.7}$$

$$v_{i+r,j+s,k+t} - v_{i,j,k} > k'\Delta df \tag{2.8}$$

In order to maintain the velocity trend and only reduce the velocity difference, their adjusted values are

$$\begin{aligned} v_{i+r,j+s,k+t} = \quad & \frac{v_{i+r,j+s,k+t}+v_{i,j,k}}{2} \\ & + \frac{v_{i+r,j+s,k+t}-v_{i,j,k}}{2\left|v_{i+r,j+s,k+t}-v_{i,j,k}\right|} k'\Delta df \end{aligned} \tag{2.9}$$

$$\begin{aligned} v_{i,j,k} = \quad & \frac{v_{i+r,j+s,k+t}+v_{i,j,k}}{2} \\ & - \frac{v_{i+r,j+s,k+t}-v_{i,j,k}}{2\left|v_{i+r,j+s,k+t}-v_{i,j,k}\right|} k' \times \Delta df \end{aligned} \tag{2.10}$$

In this way, the main velocity trend is preserved by maintaining the average velocity between any pair of grid velocity values the same. The larger velocity of any pair of adjacent grid points is still larger and the smaller velocity is still smaller after smoothing. Only the velocity variation is reduced to ensure that their variation honors the user-defined threshold.

CHAPTER III

MODELING EXAMPLES

3.1. Wedge Model

To test the smoothing effects with various smoothing schemes, a simple wedge model as shown in Figure 1 (a) is used here to help illustrate the smoothing results. An eikonal solver (Podvin and Lecomte, 1991) is utilized as a reference to compare to the WFC results. This eikonal solver uses a finite difference method, and its accuracy depends strongly on having a finely gridded model. As it only provides the first arrival and can not calculate multiple arrivals and amplitude, it is used here to validate the WFC first arrival results.

The wedge model is a 3D grid model with dimensions 8 km $\times$ 8 km $\times$ 8 km. The grid intervals are 400 m in each axis direction. The background blue color represents the velocity 4 km/s, and the red wedge shaped part possesses the velocity 5 km/s. There is a large velocity contrast between the boundary of these two parts. Figure 1 (b) - (d) show the smoothed model with median mesh smoothing, velocity gradient smoothing and running average smoothing respectively. In order to determine how well each smoothing scheme preserves the topological features of the original model, mean curvature smoothing is applied here to the smoothed models. As mean curvature smoothing diffuses the data mainly tangentially to the edge features, while avoiding any alterations along discontinuities (Desbrun et al., 1999; Weinkauf and Günther, 2009), the difference between the model with and without mean curvature smoothing applied are the sharp edges or noise of bivariate data. In this case, there is no noise present in the wedge model. Hence, the difference between the models with and without mean curvature smoothing can be used to describe the most important

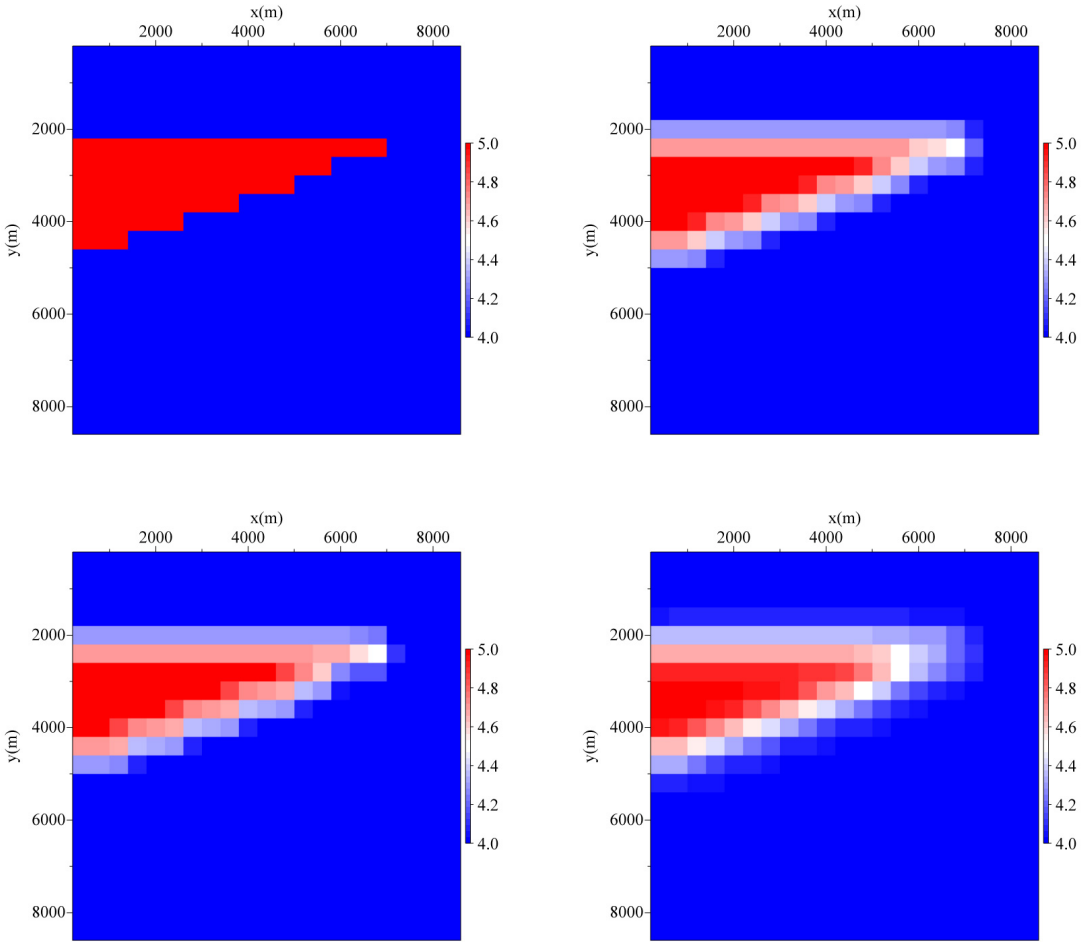

Figure 1. Cross-sctions of (a) original wedge model; (b) wedge model smoothed by median mesh filter; (c) wedge model smoothed by velocity gradient smoothing scheme; (d) wedge model smoothed by running average smoothing scheme.

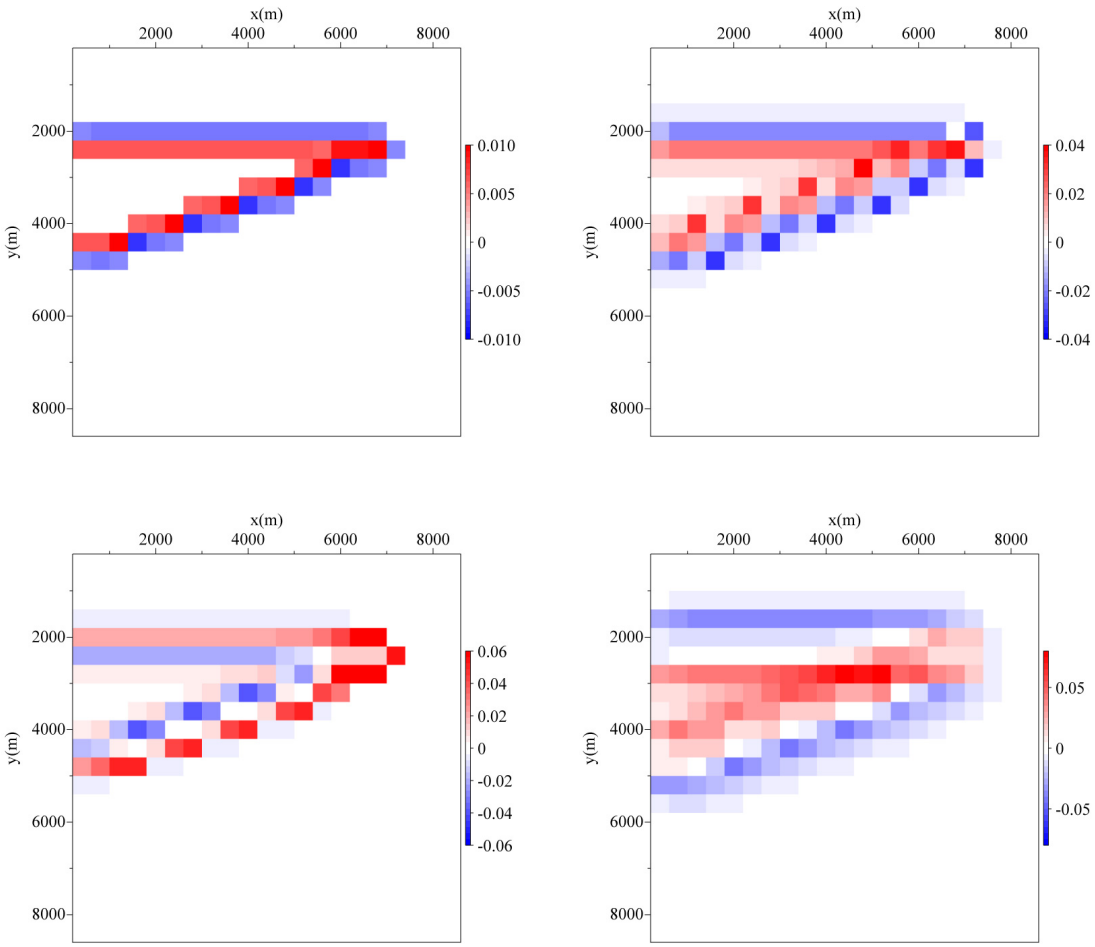

Figure 2. Edge features preserved in version of the wedge model; in each case the result of applying mean curvature smoothing is subtracted from the model to show edges. Differences for (a) original wedge model, (b) median mesh smoothed wedge model, (c) velocity gradient smoothed model, and (d) running average smoothed wedge model.

features of each model. Specifically, this approach does not strongly affect the velocity distributions, but it can effectively extract the primary edges for each model as shown in Figure 2. These figures show the topological skeletons for the original wedge model, the median mesh smoothed model, the velocity gradient smoothed model and the running average smoothed model by subtracting the corresponding mean curvature smoothed versions from each. The more similar the topological skeletons of smooth model to the original one as in Figure 2 (a), the better the associated smoothing scheme preserves the geometric features. By comparing these detected interfaces, it is clear that median mesh smoothing and velocity gradient smoothing results retain the model structure well, while the running average smoothing smears the interface around and tends to over smooth the model.

Figure 3 shows the first arrival calculated by the eikonal solver in the original unsmoothed wedge model, median mesh smoothed model, velocity gradient smoothed model and the running average smoothed model. Figure 4 illustrates the difference between the eikonal solver times from the original model and the median mesh smoothed model, the difference between times for the original model and the velocity gradient smoothed model, and the difference between times for the original model and running average smoothed model. Since the only difference in these calculations is the method of smoothing applied to each input 3-D grid model, the results illustrate how significantly the smoothing method affects traveltimes. The smaller the difference for the different models, the more similar the models are, both in velocity distribution and topological structures. Observing these differences, the first arrival difference is the smallest for the velocity gradient smoothed model, while the difference for the running average smoothed model is the largest among the three. The differences also confirm that the velocity gradient smoothing maintains the model structure well, while the running average introduces relatively large changes to the model.

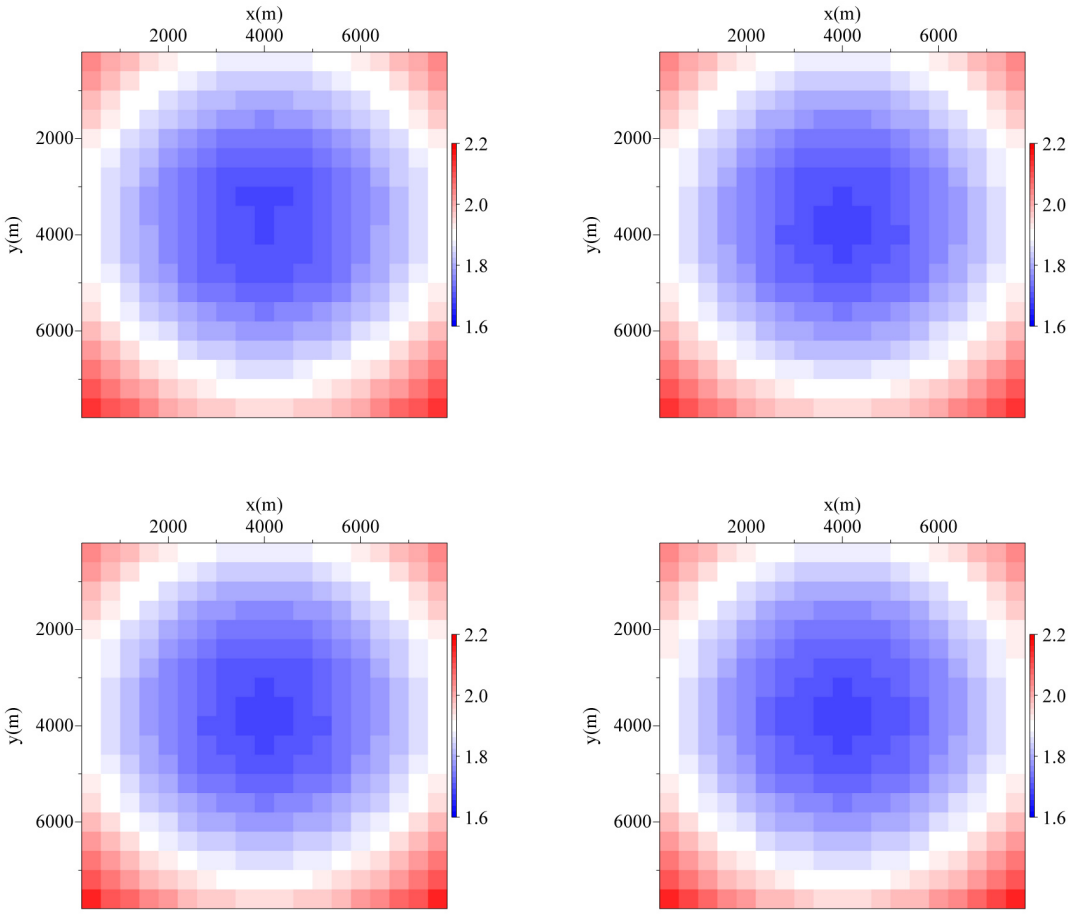

Figure 3. First arrival travel-time computed by Eikonal solver using (a) original wedge model, (b) median mesh smoothed wedge model, (c) velocity gradient smoothed wedge model, (d) running average smoothed wedge model.

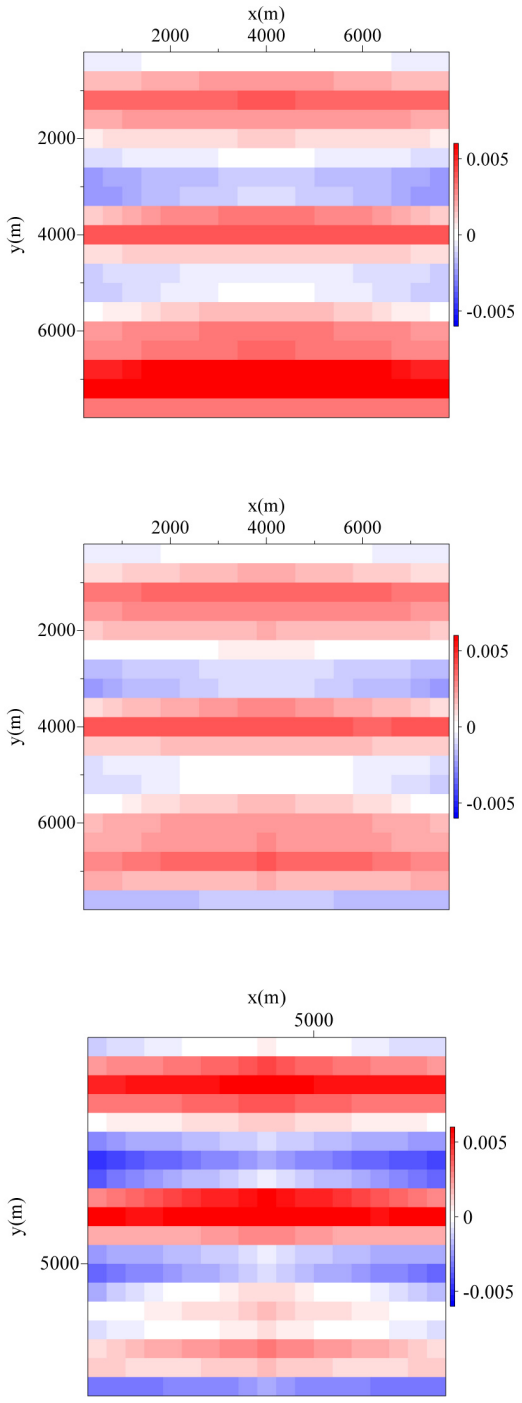

Figure 4. Differences between first arrival traveltimes computed with the eikonal solver for the original model and for (a) the median mesh filter smoothed model, (b) velocity gradient smoothing, and (c) running average smoothing.

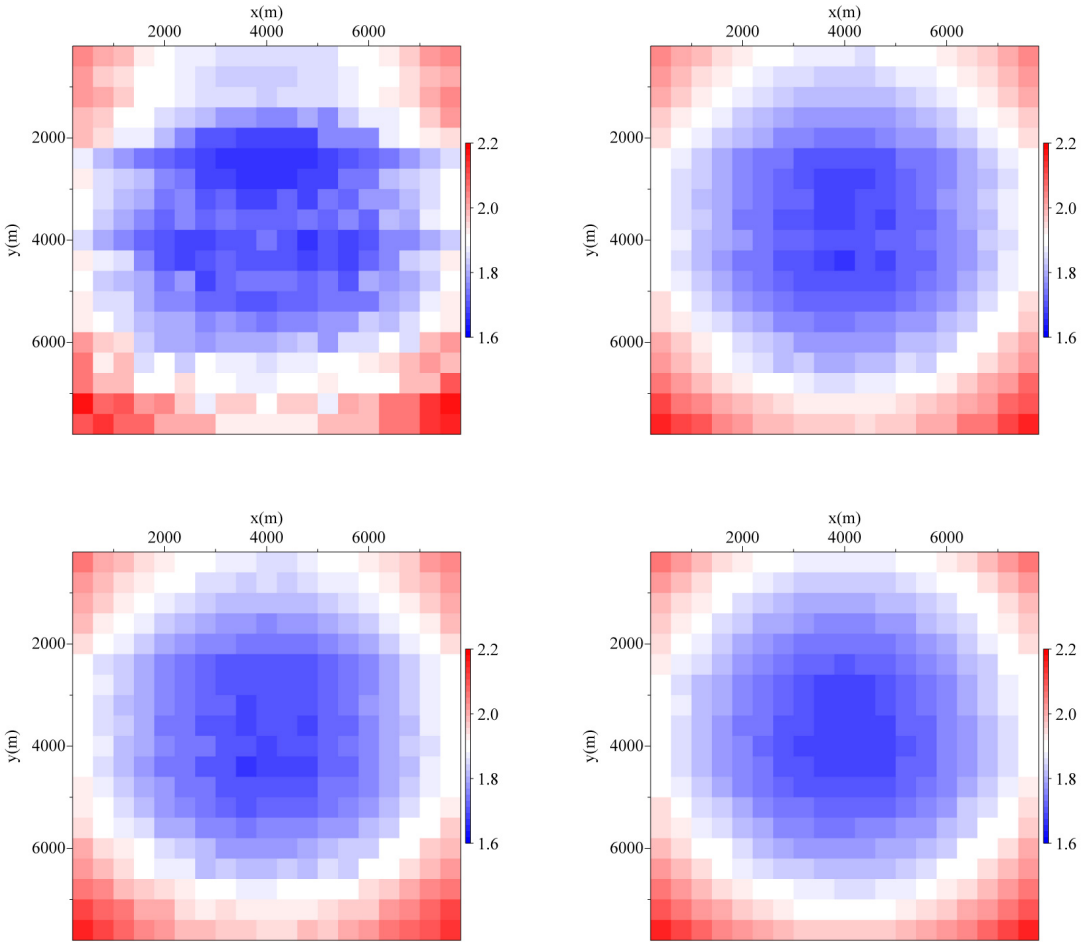

Figure 5. First arrival travel-time computed by WFC using (a) original wedge model, (b) median mesh smoothed wedge model, (c) velocity gradient smoothed wedge model, (d) running average smoothed wedge model.

With this general insight into the effects of the smoothing methods, we then apply the WFC algorithm to each of them. Since the WFC implicitly requires the smoothness constraint, it requires a certain degree of smoothing to avoid chaotic ray behavior and also to obtain more accurate computation results. Figure 5 (a) is the first arrival travel time computed by WFC using the original unsmoothed model. Comparing Figure 5 (a) - (d), one can see that the first arrival traveltime computed by WFC using the unsmoothed model (Figure 5 (a)) presents larger fluctuations and more chaotic behavior than the first arrival traveltime computed by WFC using smoothed model as in Figure 5 (b) - (d). Furthermore, the first arrival traveltime computed by WFC using smoothed model shows more similarity to the first arrival traveltime computed by Eikonal solver by comparing Figure 5 and Figure 3. Hence, the first arrival computed by WFC using the unsmoothed model is not as accurate as the one using smoothed model. It confirms the necessity of smoothing the model for ray methods. The first arrival traveltime computed by WFC using median mesh smoothing (Figure 5 (b)), velocity gradient smoothing with $k = 15\%$ and $k' = 0.1k$(Figure 5 (c)), and running average smoothing over $3 \times 3 \times 3$ smoothing cube (Figure 5 (d)) show similar results. From the parameter selection point of view, it is important to note that it is easier to select parameter k when using the velocity gradient smoothing scheme than to select the smoothing cube size for the running average. Because k measures the ratio of velocity difference to average velocity, it is more physically meaningful, while the ideal smoothing cube size is harder to relate to the velocity variations. In the velocity gradient smoothing scheme, $k = 25\%$ or less observes ray methods' smoothness requirements and is a good choice for WFC application. The parameter k is also a measurement of the smoothness degree of the model based on users' preference. The smaller the k, the smoother the model. The larger the k, the more detailed features are preserved in the smooth model. On the contrary, the smoothing cube size is

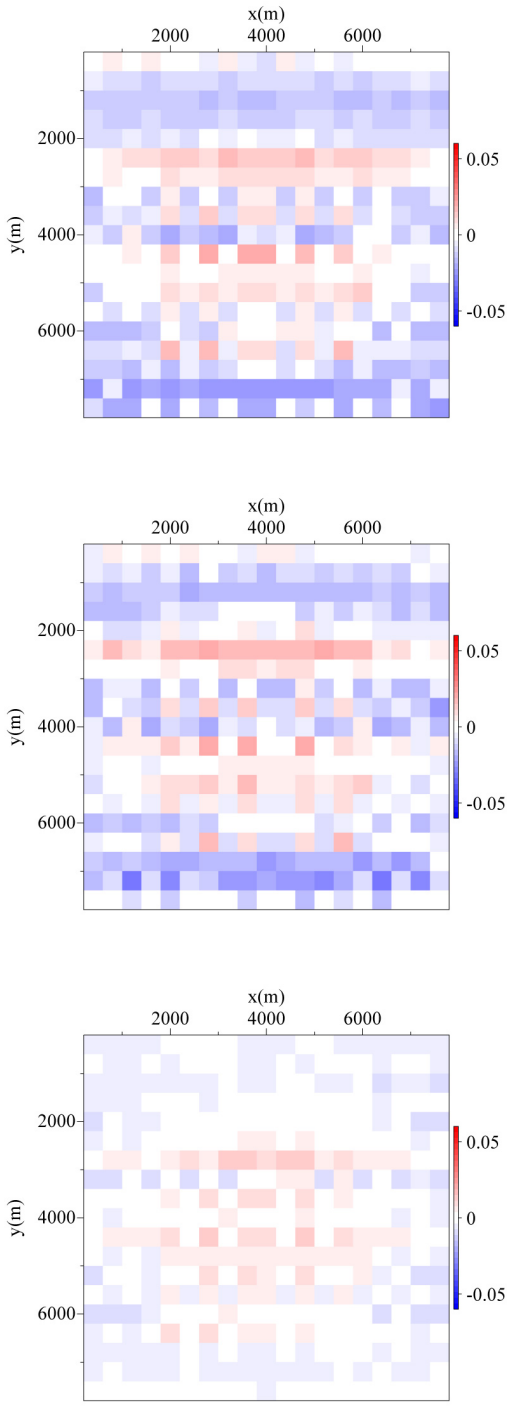

Figure 6. Differences between first arrival traveltimes computed with the eikonal solver and results from WFC for (a) the median mesh filter smoothed wedge model, (b) the velocity gradient smoothed wedge model, and (c) the running average smoothed wedge model.

decided through testing for running average smoothing scheme. Here the smallest smoothing cube size $3 \times 3 \times 3$ is sufficient. However, in some other models, these parameters may not be able to generate a smooth enough model and need adjustment via trial and error. Figure 6 presents the difference between the Eikonal solver and WFC using the three smoothing methods respectively. The almost-zero difference supports the good agreement between the WFC alogrithm and the Eikonal solver.

Because the eikonal solver cannot compute amplitude and multiple arrivals, such results from WFC computations cannot be tested using it. Figure 7, however, shows the amplitudes generated by WFC using the median mesh smoothed model, the velocity gradient smoothed model, and the running average smoothed model, respectively, to show how smoothing changes these values too. The amplitude using the median mesh smoothed model (Figure 7 (a)) and the one using the velocity gradient smoothed model (Figure 7 (b)) are the most similar among the three. It infers that these two models are more similar to the original model than the running average smoothed one.

3.2. 3-D Implementation of Marmousi Model

The Marmousi model (Versteeg and Grau, 1991) is a more complex, strongly heterogeneous model that tests interpolation and smoothing schemes. The original Marmousi model, which is based on a profile through the North Quenguela trough in the Cuanza basin, is a very complex 2-D model (Figure 8 (a)). It contains strong horizontal and vertical velocity gradients, and reliable imaging of synthetic seismograms would require advanced processing techniques. The dimensions of the model are 9200 m (length) by 3000 m (depth). Values of velocity, which correspond to P waves, are specified at a grid spacing of 4 m in each direction. Velocity varies from

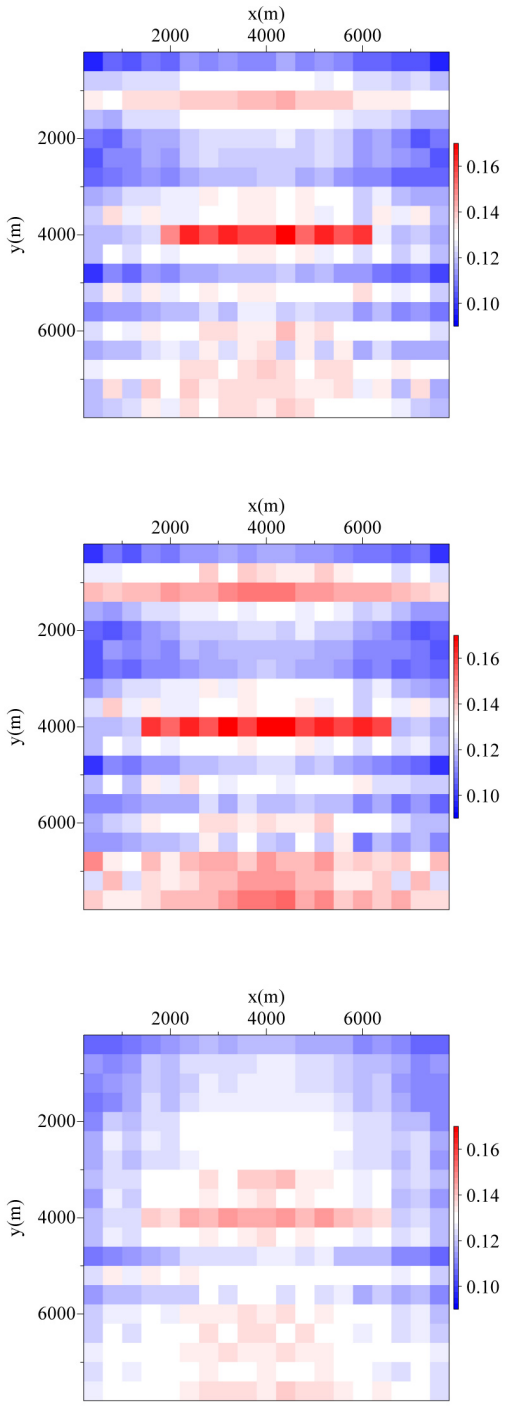

Figure 7. First arrival amplitude computed by WFC for the (a) median mesh smoothed wedge model, (b) velocity gradient smoothed wedge model, and (c) the running average smoothed wedge model.

1500 m/s to 5500 m/s.

We extend the Marmousi model in the third dimension to generate a 3-D model. Its vertical slice along the $y-z$ plane is the same as Figure 8 (a), and the properties are then constant in the x direction. Comparisons of the results of velocity gradient smoothing and running average smoothing are presented in Figure 8 (b) and Figure 8 (c). The eikonal solver provides an alternate solution to verify and test results as in the previous wedge example.

Figure 9 displays velocity as a function of depth at x=2000 m, y=7000 m in the original 3D extended Marmousi model and in the smoothed Marmousi models using running average and velocity gradient smoothing schemes. The running average smoothing applied the filter over a $9\times9\times9$ smoothing cube, while the velocity gradient smoothing utilized a value of $k = 15\%$. One can see that the result of the velocity gradient smoothing scheme (red line), follows the trend of the original velocity (green dashed line), better than the values from the running average (blue line). Local maxima and minima remain in the same spatial positions in the velocity gradient smoothed model, though variations are smoothed.

By applying the mean curvature smoothing, the structural features can be extracted from the original model, the velocity gradient smoothed model and the running average smoothed model (Figure 10). Comparing these three plots, one can see that the velocity gradient smoothing retains more structural details than running average smoothing, although both of these two models satisfy the smoothing requirement of ray method. Additional insights are provided by the first arrival traveltime computed by the eikonal solver using these three models (Figure 11) and their differences (Figure 12). The first arrival using velocity gradient smoothed model (Figure 11 (b)) shows more similar patterns to the original model (Figure 11 (a)) than the running average smoothing (Figure 11 (c)). This can be confirmed by the histogram

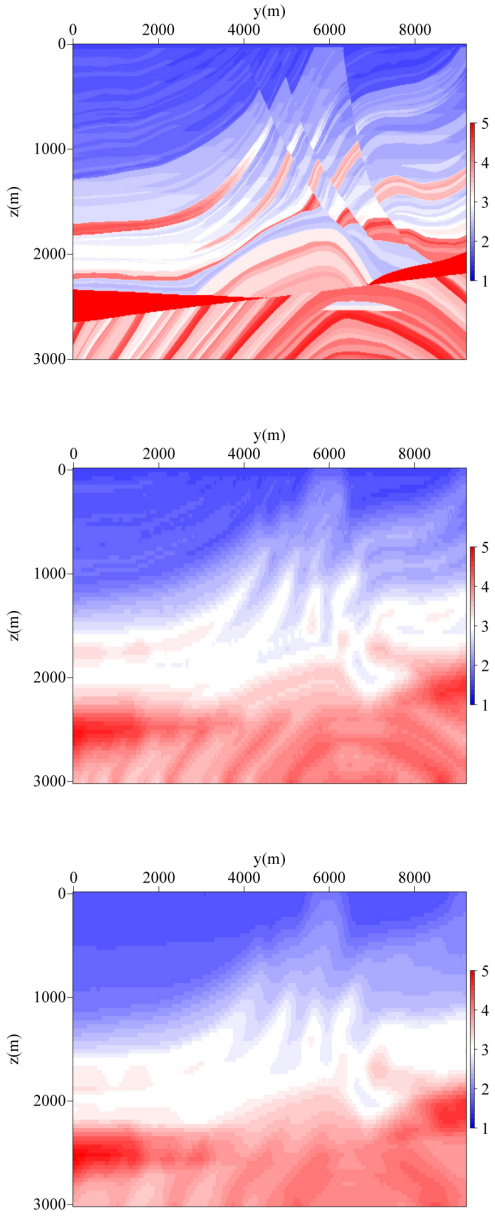

Figure 8. Vertical cross sections through the (a) original Marmousi model; (b) the velocity gradient smoothed Marmousi model and (c) the running average smoothed Marmousi model.

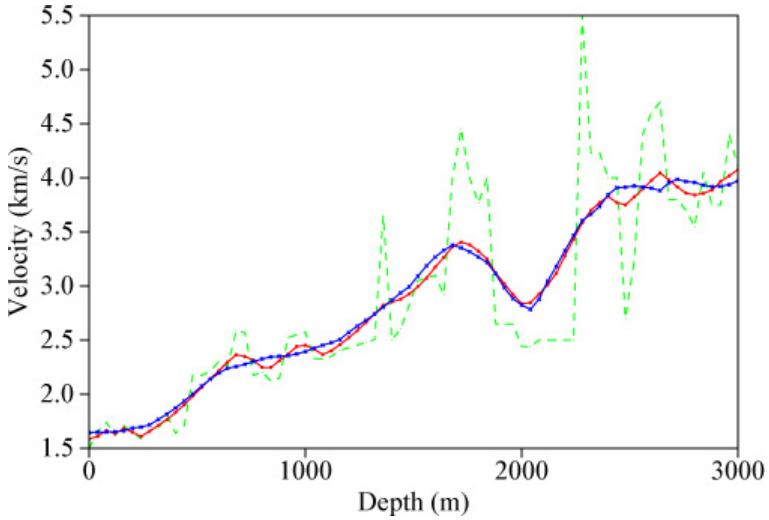

Figure 9. Velocity variation with depth at x=2000m, y=7000m of 3D Marmousi model. Green dash line represents the original velocity of Marmousi Model. Red and blue solid lines are the velocity after velocity gradient smoothing and running average smoothing respectively.

of their differences (Figure 13) and their mean values and standard deviations (Table I). The means and standard deviations of first arrival differences are smaller for the velocity gradient smooth model than the running average smooth model. As the only difference in computations is the input models, these differences indicate that the velocity gradient smooth model gives results closer to those for the original, unsmoothed model, and it is able to generate more accurate traveltime results than the running average smooth model.

3.2.1. WFC Traveltimes

A 2-D array of 66 × 191 receivers is uniformly distributed on the surface with an interval of 40 m in each direction to test the accuracy of wavefront construction code in the heterogeneous, isotropic model. The seismic source is located at $(x, y, z) = (1.48, 4.6, 2.8)$. Example wavefronts are also displayed in Figure 14. In order to

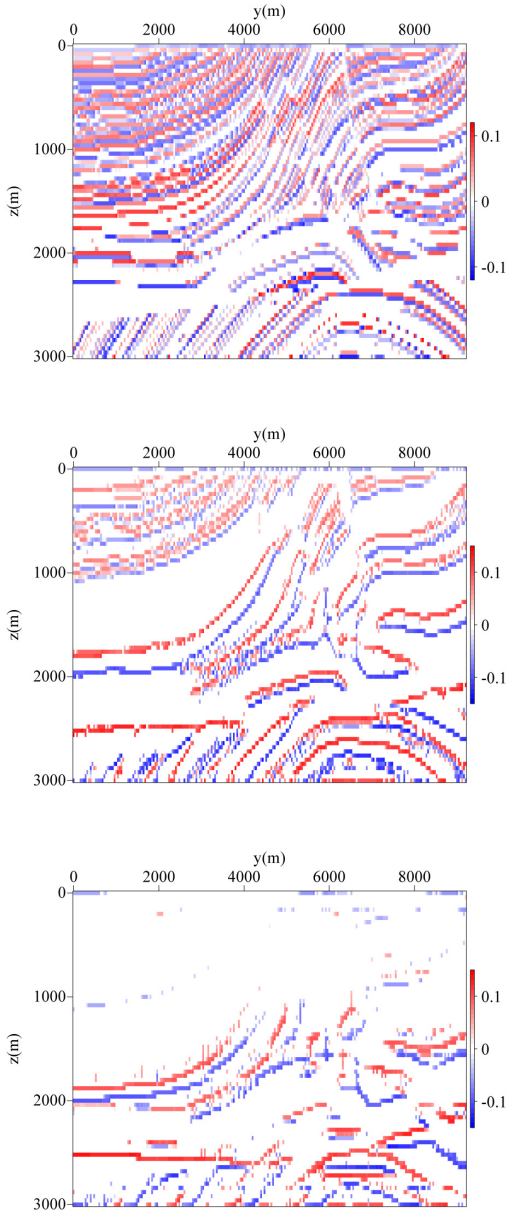

Figure 10. Edge features preserved in version of the Marmousi model; in each case the result of applying mean curvature smoothing is subtracted from the model to show edges. Differences for (a) the original model, (b) the velocity gradient smoothed model, and (c) the running average smoothed model.

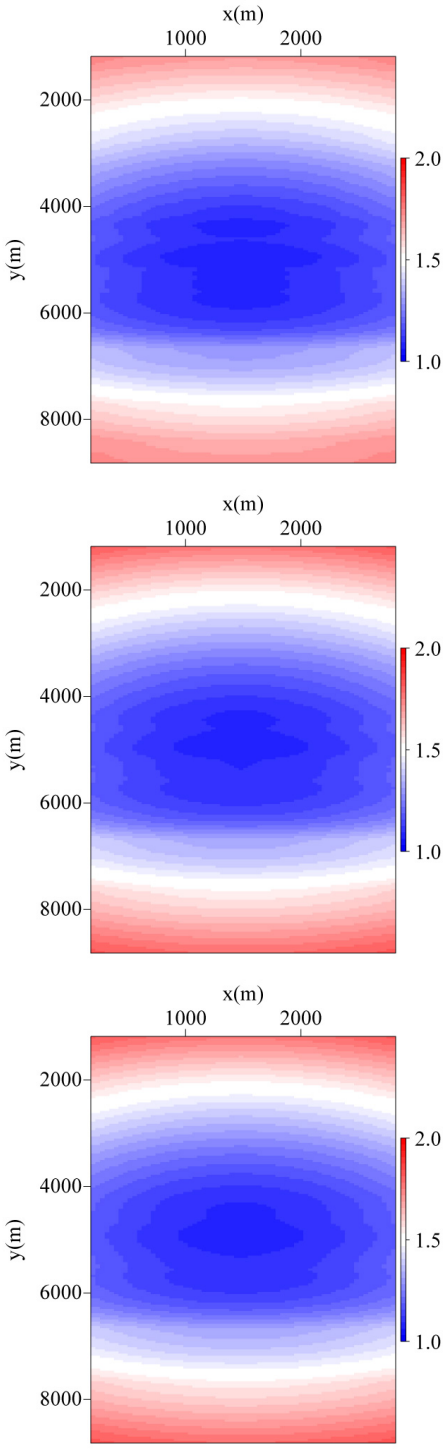

Figure 11. First arrival travel-time computed by Eikonal solver using (a) original Marmousi model, (b) velocity gradient smooth Marmousi model, and (c) running average smooth Marmousi model.

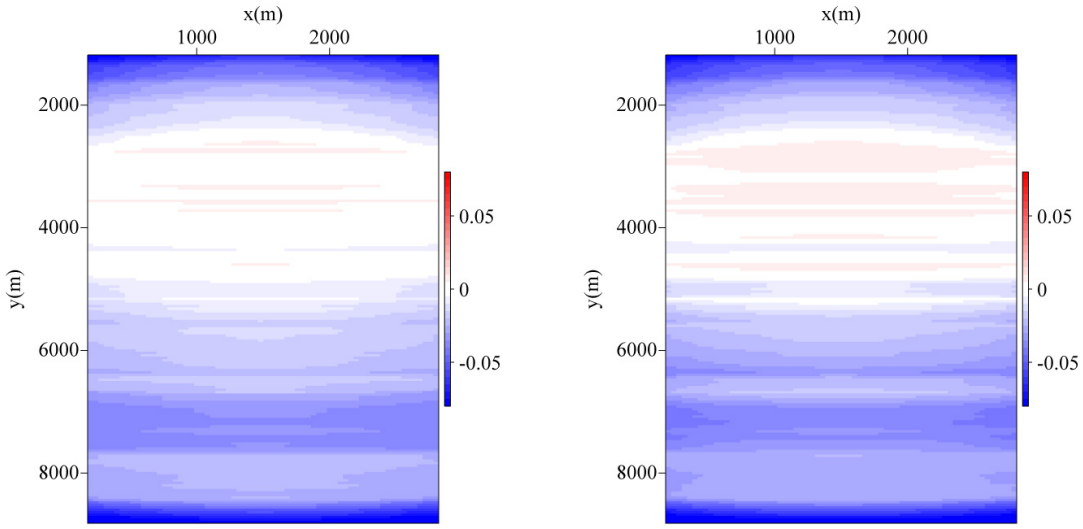

Figure 12. Difference of first arrival computed by Eikonal solver (a) between unsmoothed Marmousi model and velocity gradient smoothed one; (b) between unsmoothed Marmousi model and running average smoothed one.

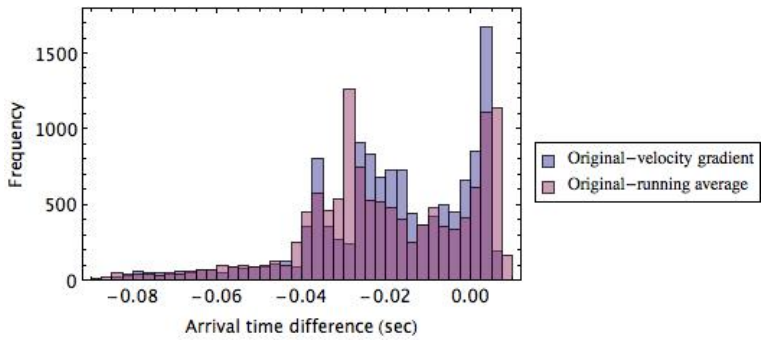

Figure 13. Distributions of first arrival traveltime differences obtained by applying the eikonal solver to the earth models in Figure 8. These differences compare the results for the original, unsmoothed velocity model to those obtained for two smoothed models. Note that the overlapping region of the two different data sets shows as dark purple, while the lighter colors show distinct regions in the plot

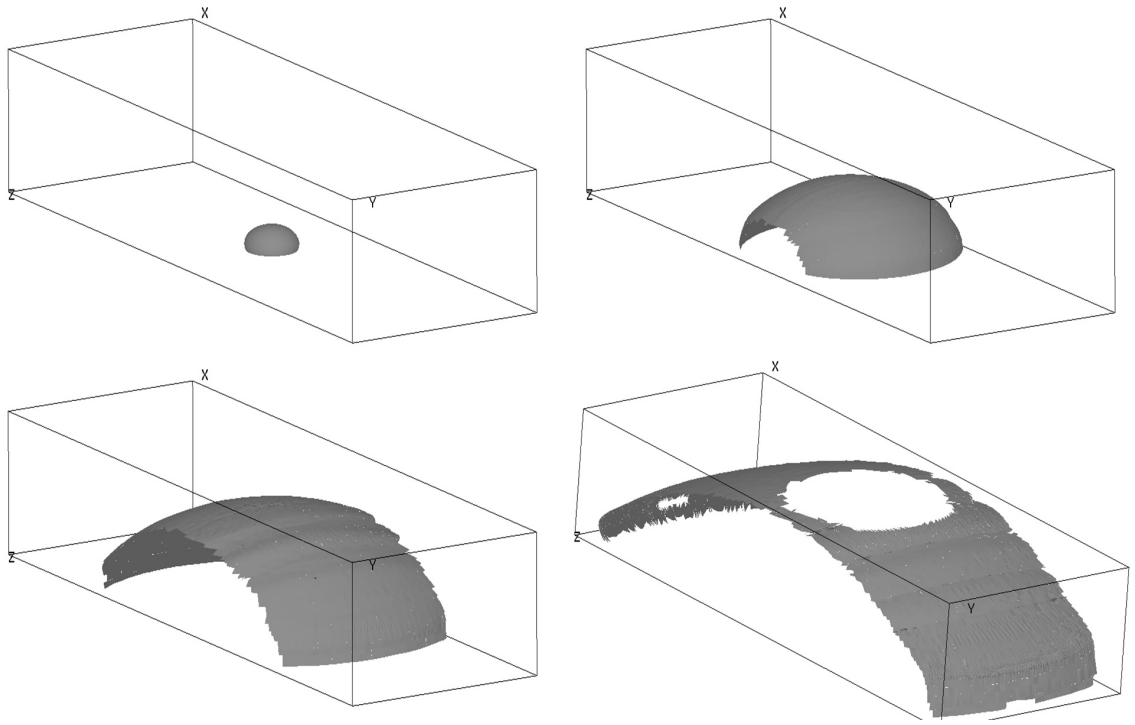

Figure 14. Simulated wavefront propagation in 3-D Marmousi model at time (a) 0 second; (b) 0.3 second; (c) 0.6 second; (d) 1 second.

compare the WFC results with the Eikonal solver results as above, the first arrivals of WFC results are selected, although WFC can generate multiple arrival traveltimes. The first arrivals using the velocity gradient model are presented in Figure 15 (a) and the first arrivals using the running average smoothed model are in Figure 15 (b). When comparing these sets of values, there are some important points to note. First, unlike the eikonal solver first arrivals computed using the unsmoothed model, these two plots are slightly asymmetric in the x direction, which is a consequence of the smoothing order in the model.

To quantify the influence of model smoothing on the WFC algorithm, these first arrival WFC results are compared with those computed by the eikonal solver using

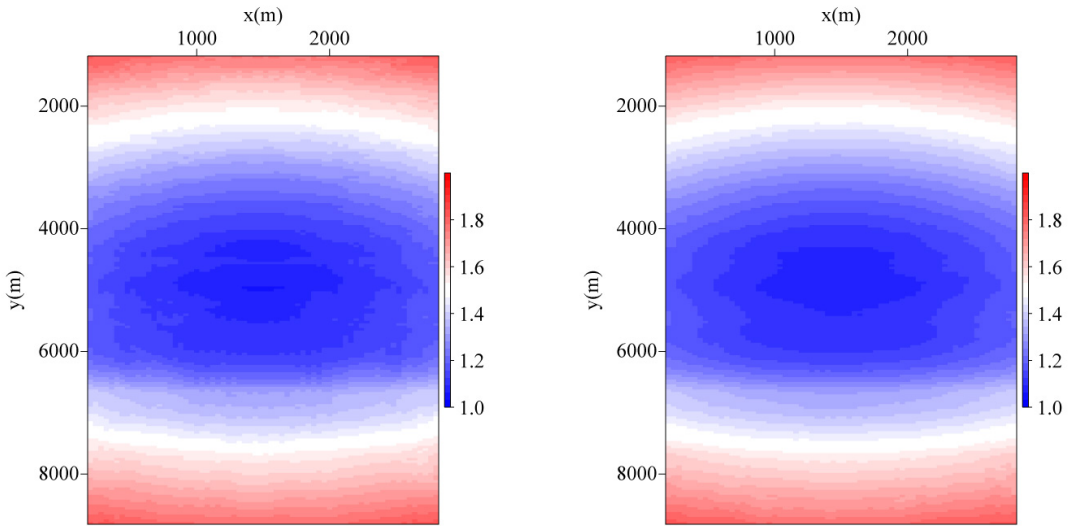

Figure 15. First arrival travel-time computed by WFC (a) using velocity gradient smoothed Marmousi model; (b) using running average smoothed Marmousi model.

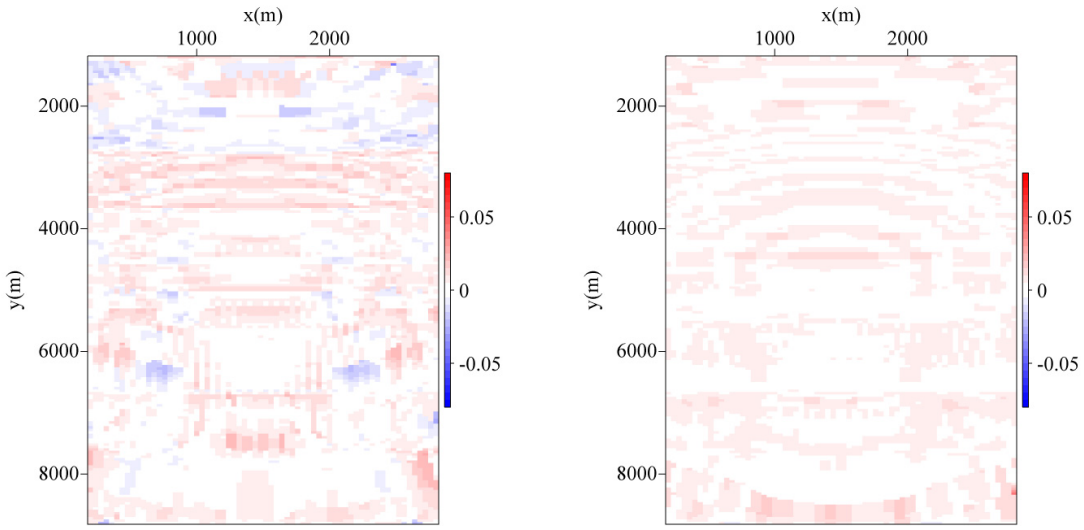

Figure 16. Difference between WFC and eikonal solver first arrival times (a) using the velocity gradient smoothed Marmousi model, (b) using the running average smoothed Marmousi model.

the same smooth models. Their differences are shown in Figure 16. In general, the traveltime differences for the running average model have a smoother spatial variation, and the extremes are smaller than those obtained for the velocity gradient case. This is likely because the running average procedure gives a smoother velocity model that is missing some of the more detailed features (Figure 10). Further insights into these differences are obtained from several statistics, such as the mean, standard deviation and median of traveltime difference values (Table II). The mean difference is smaller for the velocity gradient model, though the larger standard deviation shows the increased scatter in difference values. Medians show values similar to means, which is because the distribution of values is closer to Gaussian than for the previously examined differences obtained from the eikonal solver results (Figure 13). While the velocity gradient model does give some larger differences, in general the smaller mean difference suggests generally reliable results.

As stated before, our goal of smoothing is to obtain a smooth earth model that maintains its geometric features, because such smoothed models should be able to produce the closest travel time results to those from the original, unsmoothed velocity model. In order to show that the velocity gradient smoothing scheme does in fact generate traveltimes more similar to the values from the unsmoothed Marmousi model, we compare the Eikonal solver results from the unsmoothed model (Figure 11 (a)) to WFC results using the smoothed models (Figure 15). These differences are shown in Figure 17, and histograms of the differences are in Figure 18. The means, standard deviations and medians can be found in Table III. From the histogram (Figure 18), one can see that the values for the running average model have more local maxima at large differences, whereas the distribution is smoother for the velocity gradient results. The mean differences, however, are quite similar though the value is slightly smaller for the velocity gradient case. Although the differences between

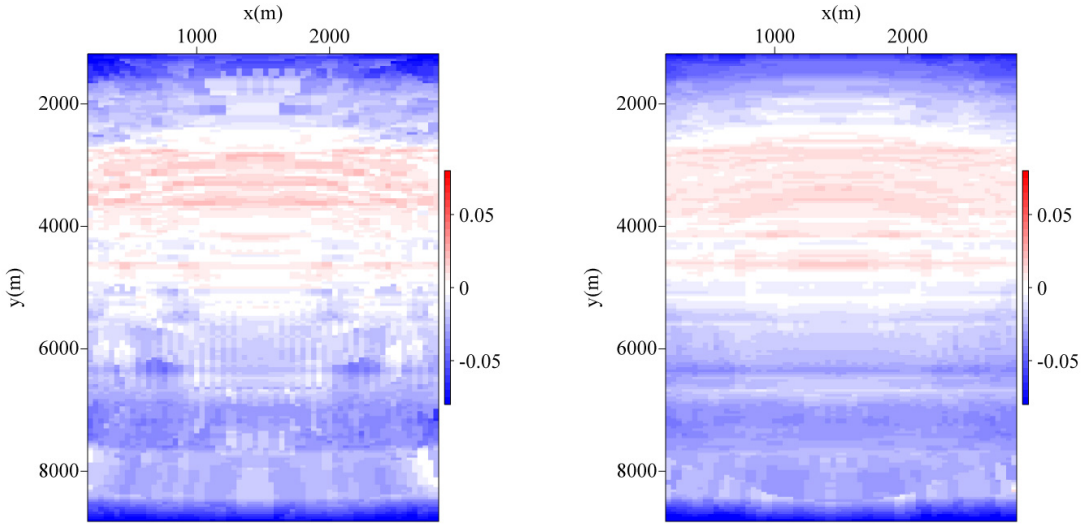

Figure 17. Difference of first arrival computed by Eikonal solver (a) between unsmoothed Marmousi model and velocity gradient smoothed one, (b) between unsmoothed Marmousi model and running average smoothed one.

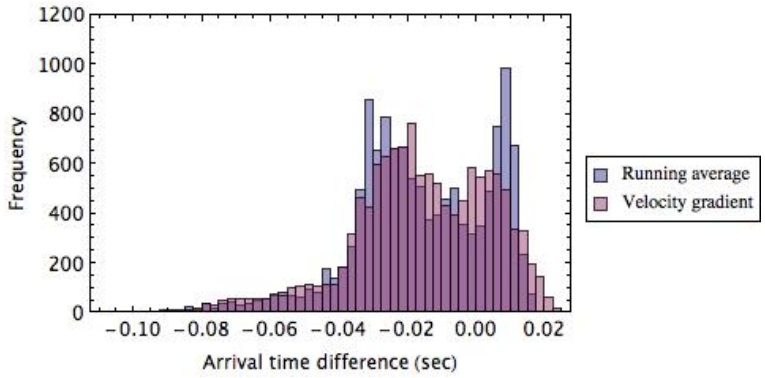

Figure 18. Histograms showing distribution of differences in arrival times computed using eikonal and WFC methods for two different smoothed models. Note that the overlapping region of the two different data sets shows as dark purple, while the lighter colors show distinct regions in the plot.

smoothing methods here are relatively small, combining these with previous results suggests that the velocity gradient smoothing model results in traveltime behavior that is at least as good as the running average approach or sometimes better. For this reason, it should be the better choice for a smoothing algorithm.

Table I. Means, standard deviations and medians of differences in eikonal solver first arrival traveltimes for the Marmousi model. Each row compares values from the unsmoothed model to those from a smoothed model.

Model	Mean	Standard Deviation	Median
Running average	-0.0198	0.0199	-0.0210
Velocity gradient	-0.0185	0.0186	-00177

Table II. Means, standard deviations and medians of differences between eikonal and WFC first arrival times computed for smoothed models. Each row compares values for the different numerical approaches as applied to the specified model.

Model	Mean	Standard Deviation	Median
Running average	0.00399	0.00314	0.00385
Velocity gradient	0.00274	0.00662	0.00293

3.2.2. Multivalued Traveltime Fields and Amplitudes

In additional to computing the first arrival, as does the eikonal solver, WFC is able to simulate multiple arrivals, which are important for true-amplitude migration, velocity model updates and other applications. The number of arrivals are counted at

Table III. Means, standard deviations and medians of differences between first arrivals from WFC for a smooth model and results from the eikonal solver applied to the original Marmousi model.

Model	Mean	Standard Deviation	Median
Running average	-0.0158	0.0198	-0.0169
Velocity gradient	-0.0157	0.0201	-0.0157

each receiver as shown in Figure 19 for velocity gradient model and running average smoothed model respectively. The multiple arrivals mainly comes from the triplications caused by the velocity variations in the model. The velocity gradient model shows more complicated pattern of arrival numbers and overall it has larger arrival numbers than running average model, which indicates that the structure in velocity gradient model is more complicated than the running average smoothed model.

Amplitudes are generated to demonstrate the WFC algorithm can simulate the wavefront propagation in triplication zones correctly. Again, the same source receiver geometry and model are used. Because the analytic solutions for amplitudes are not available for the eikonal solver, we showed the plots of all arrivals' amplitudes as Figure 20 instead of their errors. The amplitude of multiple arrivals are expected to be higher than its surrounding amplitudes due to its higher ray density than its surroundings. By comparing Figure 19 and Figure 20, one can see that the high amplitude zones in Figure 20 correspond to the multiple arrival zones in Figure 19. It confirms that WFC can record multiple arrivals and their amplitudes.

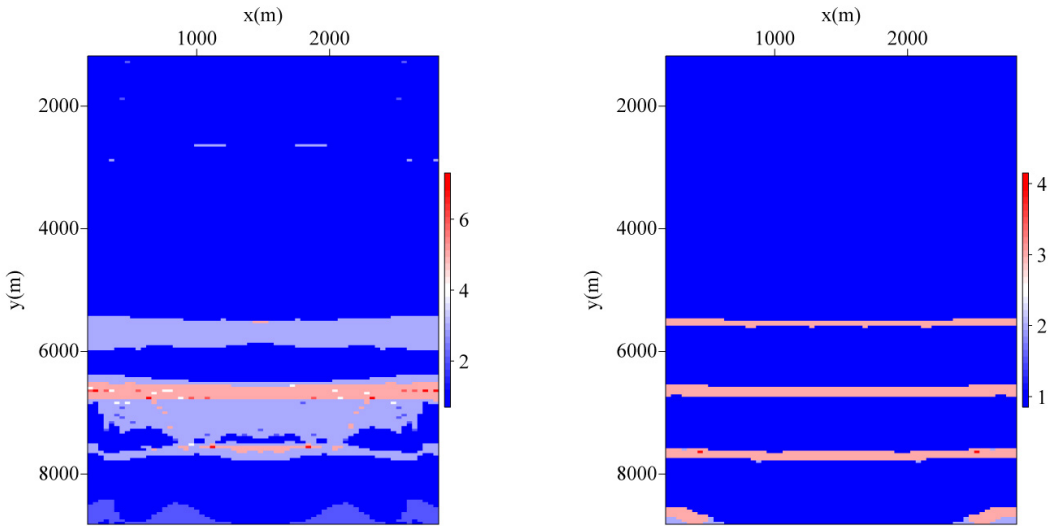

Figure 19. Number of arrivals at each receiver location from (a) the velocity gradient smoothed Marmousi model, (b) the running average smoothed Marmousi model.

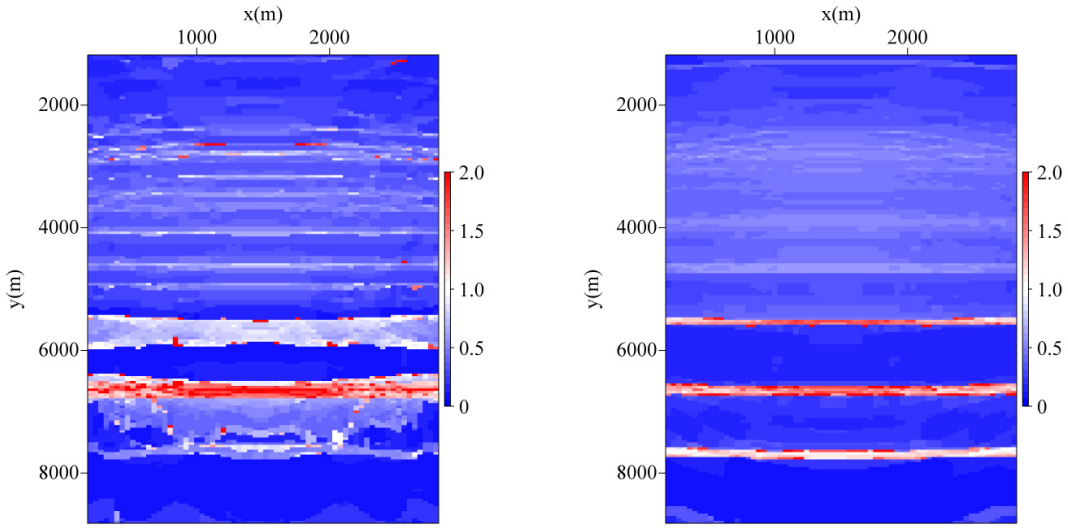

Figure 20. First arrival amplitudes from WFC for (a) the velocity gradient smoothed Marmousi model, and (b) the running average smoothed Marmousi model.

CHAPTER IV

DISCUSSION

In order to analyze the behavior of the proposed velocity gradient smoothing scheme and verify the performance of WFC in 3D gridded earth models, a simple wedge model and a fairly complicated 3D extended Marmousi model were tested.

The importance of smoothing in WFC applications was shown first by applying an unsmoothed wedge model directly to the WFC algorithm, with results that are unreliable. Then three smoothing schemes were compared, namely the median mesh smoothing, velocity gradient smoothing and running average smoothing. Comparing the implementations of the various approaches, it is important to note that there are important distinctions in the ease of parameterizing them. For example, the median mesh smoothing is sensitive to the radius value, as a larger smoothing radius leads to model feature distortions. Therefore, although it gives decent modeling results in the wedge model, it was not further tested. The parameter k in velocity gradient smoothing is defined as the ratio of velocity change within half the wavelength to the average velocity under consideration. It is directly related to the velocity variations in the earth model and is straightforward for users to choose. Considering the running average smoothing, its primary parameter, the smoothing cube size, depends strongly on the grid interval, 400 m for the wedge model. The smallest smoothing cube size $3 \times 3 \times 3$ is applied here, with 1 grid point included in each direction centered on the smoothed grid point, but it still oversmooths the model and gives inaccurate travel-time results compared with median mesh smoothing and velocity gradient smoothing.

Similar test procedures are carried out on the 3D extended Marmousi model. Here it only compares the velocity gradient smoothing with the running average smoothing. Likewise, the smoothness for these two schemes are designed to be as

similar as possible to allow a fair comparison. However, unlike velocity gradient smoothing, running average smoothing replaces each grid point value with the average of the smoothing cube values and does not adaptively detect the velocity contrast. Therefore, there are places where running average smoothed model is more or less smooth than the velocity gradient smooth model. First, the capability of feature preservation is compared by checking the velocity change with depth as Figure 9 and extracting the geometric skeletons of the model as Figure 10. The comparison verifies that velocity gradient smoothing scheme better follows the trend of velocity variation and better preserves the features in the model.

It is also important to consider which smoothing scheme can help generate a more accurate modeling result. In order to do so, an Eikonal solver, which can tolerate large velocity contrast but can only compute first arrival traveltimes, is utilized as a reference to compare its first arrival results with the WFC results. There are mainly three types of differences that provide insights into the influence of smoothing and accuracy of results. The first is the difference between the Eikonal solver result using the original unsmoothed model and the smoothed model. Since they all use the same Eikonal solver algorithm, and the only difference is the model, the difference shows the similarity of the smoothed model to the original model. The smaller the difference, the more similar the smoothed model is to the original model in terms of traveltime behavior. Based on the analysis in the above section and the difference in Figure 12, the difference for velocity gradient smoothing is smaller than that of running average smoothing. Hence, it confirms again the velocity gradient smoothing can generate a smoothed model that is more similar to the original model. The second type of difference is between the Eikonal solver results and WFC results using the same smoothed model as Figure 12. Since the models are the same, although computed with different algorithms, the first arrivals are expected to be the same or at least very

similar. The test difference agrees with this and confirms that the smoothed models are smooth enough for WFC applications and the competitive performance of WFC using the 3D grid models. The third type of difference is between the Eikonal solver results using original unsmoothed model and WFC results using smoothed models as Figure 17. This is used to assess the performance of the WFC algorithm and the contribution from different smoothing schemes to the accurate modeling results. The smaller difference for velocity gradient smooth model verifies that velocity gradient smoothing helps WFC to generate more accurate traveltimes than running average smoothing. Additionally, by comparing the first type of difference and the third type, one can suggest that the WFC can generate first arrival results using smoothed model that are closer to the results of the original model than Eikonal solver itself.

CHAPTER V

CONCLUSION

A 3-D grid model is introduced to the WFC method. Smoothing and parameter interpolation schemes are investigated and solved to achieve this and enhance WFC performance. The velocity gradient smoothing scheme is implemented in the WFC algorithm, and it makes the grid model smooth enough to satisfy the asymptotic assumption of ray tracing and also reserve the geological features inherited in the original grid model. An improved inverse distance weighting interpolation scheme is also applied to quickly and accurately estimate the elastic parameters at arbitrary locations based on the prescribed property values on the grid points. The test results validate the feasibility of smoothing and interpolation methods proposed in this paper and the improvements on the computation accuracy and efficiency WFC method has achieved.

REFERENCES

Alde, D. M., Fehler, M. C., Hildebrand, S. T., Huang, L. and Sun, H., 2002. Determining the optimally smoothed slowness model for ray-tracing based migration using multiple-valued travel-time tables. SEG Expanded Abstracts, **21**, 1168.

Bulant, P., 2002: Sobolev scalar products in the construction of velocity models: Application to model Hess and to SEG/EAGE Salt Model. Pure and Applied Geophysics, **159**, 1487-1506.

Carcione, J. M., Herman, G. C., ten Kroode, A. P. E., 2002. Seismic modeling. Geophysics, **67**, 1304-1325.

Červený, V., Horn, E., 1980, The ray series method and dynamic ray-tracing system for three-dimensional inhomogeneous media. Journal of Geophysical Research, **89**, 1466-1494.

Červený, V., Soares, J. E. P., 1992. Fresnel volume ray tracing. Geophysics, **57**, 902-915.

Červený, V., 2001, Seismic ray theory. New York: Cambridge University Press.

Coman R, Gajewski D., 2001. Estimation of multivalued arrivals in 3-D models using wavefront ray tracing. 71st Annual International Meeting, Society of Exploration Geophysicists. Expanded Abstracts, 1265-1268.

Desbrun, M., Meyer, M., Schŕoder, P., and Barr, A.H., 1999, Implicit fairing of irregular meshes using diffusion and curvature flow. Proceedings of SIGGRAPH, 317-324.

Fehler, M. C., Huang, L., 2002. Modern imaging using seismic reflection data. Annual Review of Earth Planetary Sciences, **30**, 259-284.

Gajewski, D., and Vanelle, C., 2002, Amplitude-preserving Kirchhoff migration: A traveltime-based strategy. Studia geophysica et geodaetica, **46**, 193-211.

Gibson, R. L. Jr., Durussel, V. D., and Lee, K. J., 2005, Modeling and velocity analysis with a wavefront construction algorithm for anisotropic media: Geophysics, **70**, 63-74.

Gjøystdal, H., Iversen E., Lecomte, I., Kaschwich, T., Drottning, A., and Mispel, J., 2007, Improved applicability f ray tracing in seismic acquisition, imaging, and interpretation: Geophysics, **72**, 261-271.

Gray, S., 2000, Velocity smoothing for depth migration: How much is too much?, 70th Annual International Meeting: Society of Exploration Geophysicists, 1055-1058.

Hale, D., 2009, Structure-oriented smoothing and semblance. Appeared in 2009 Project Review, CWP-636.

Kravchenko, A. N., 2003, Influence of spatial structure on accuracy of interpolation methods. Soil Science Society of America Journal, **67**, 1564-1571.

Kravtsov, Y. A., Orlov, Y. I., 1990. Geometrical optics of inhomogeneous media. Berlin: Springer-Verlag.

Lai, H.L., Gibson, Jr., R. L., and Lee, K.J., 2009. Quasi-shear wave ray tracing by wavefront construction in 3-D, anisotropic media: Journal of Applied Geophysics, **69**, 82-95.

Lee, K.J. and Gibson, Jr., R. L., 2007. An improved mesh generation scheme for the wavefront construction method: Geophysics, **72(1)**, T1-T8.

Massopust, P. R., 2010. Interpolation and approximation with splines and fractals. New York : Oxford University Press.

Nielson, G: 1993, Scattered data modeling, IEEE Computer Graphics and Applications, **13**, 60-70.

Pacheco, C. and Larner, K., 2005. Velocity smoothing before depth migration: Does it help or hurt? SEG/Houston 2005 Annual Meeting, Expanded Abstracts, 1970 - 1974.

Podvin, P., Lecomte, I., 1991. Finite difference computation of traveltimes in very contrasted velocity models: A massively parallel approach and its associated tools. Geophysics, **105**, 271-284.

Shepard, D.D., 1968, A two dimensional interpolation function for irregularly spaced data. Proceedings of 23rd National Conference ACM, 517-524.

Versteeg, R., and Grau, G., 1991, The Marmousi experience. Proceedings of EAEG workshop on Practical Aspects of Seismic Data Inversion EAEG, 516.

Vinje, V., Iversen, E., and Gjøtdal, H., 1993, Traveltime and amplitude estimation using wavefront construction. Geophysics, **58**, 1157-1166.

Vinje, V., Iversen, E., Åstebøl, K., and Gjøstdal, H., 1996. Estimation of multivalued arrivals in 3D models using wavefront construction - Part I, Geophysical Prospecting, **44**, 819-842.

Vinje, V., 1997, A new interpolation criterion for controlling accuracy in wavefront construction. Expanded Abstracts of 67th SEG Annual Meeting (Dallas): Society of Exploration Geophysicists, Tulsa. 1723-1726.

Weinkauf, T., Günther, D., 2009. Separatrix persistence: Extraction of salient edges on surfaces using topological methods. Eurographics symposium on geometry processing, **28(5)**, 1519-1528.

Žáček, K., 2002. Smoothing the Marmousi model. Pure and Applied Geophysics, **159**, 1507-1526.

APPENDIX A

KEY RESULTS FOR SEISMIC RAY TRACING

The WFC method is an implementation of the standard ray tracing method that aims to simulate the explicitly track the propagation of entire wavefronts instead of individual rays. At a given time, the ray points are connected and form a wavefront. New rays are inserted when the ray field diverges and certain interpolation criteria are violated. The ray paths and travel times for general anisotropic media can be derived by integrating the right hand side of a set of ordinary differential equations in the form (Gibson et al., 2005)

$$\frac{dx_i}{d\tau} = a_{ijkl} p_l g_j g_k \tag{A.1}$$

$$\frac{dp_i}{d\tau} = -\frac{1}{2}\frac{da_{ijkl}}{dx_i} p_n p_l g_j g_k \tag{A.2}$$

$$a_{ijkl} = \frac{c_{ijkl}}{\rho} \tag{A.3}$$

Here, x_i are spatial coordinate components, p_i are slowness vector components, τ is travel time, a_{ijkl} are density normalized elastic moduli (stiffness tensor), and g_i are eigenvectors of Christoffel matrix, Γ_{ij},

$$(\Gamma_{jk} - v^2 \delta_{jk}) u_k = 0, \tag{A.4}$$

$$\Gamma_{jk} = a_{ijkl} p_i p_l \tag{A.5}$$

where v is a phase velocity in the direction of p_i and we have three eigenvalues for each squared phase velocity. The travel time along a ray path can be found by solving the right hand side of $dx_i/d\tau$ in equation A.1.

APPENDIX B

IMPROVED INVERSE DISTANCE WEIGHTING INTERPOLATION

The conventional IDW is broadly recognized and employed as the basic method in a lot of geoscience applications. Given any arbitrarily spaced points $u_1, u_2, \ldots, u_N \in \Re^n$ and values $f(u_1), f(u_2), \ldots, f(u_N)$ of a function f, the conventional IDW (Shepard, 1968) is given by

$$S_p^0 f(u) = \sum_{i=1}^{N} f(u_i) \cdot W_i(u), \tag{B.1}$$

where $W_i(u)$ is the weighting function,

$$W_i(u) = \frac{\|u - u_i\|^{-p}}{\sum_{j=1}^{N} \|u - u_j\|^{-p}} \tag{B.2}$$

Here p is the power factor and $\|\cdot\|$ is the Euclidean norm.

However, the 'bull's eyes' phenomenon limits its accuracy. It can be eliminated by replacing $F(u_i)$ with a suitable local approximation Q_i (Nielson 1993). In this paper, first order Taylor polynomials are applied, f's approximations of degree q at these interpolating points, so that they can mimic the shape of F_i under the condition that the distant points don't influence Q_i too much. The generalized Shepard's global formula is

$$S_p^q f(x) = \sum_{i=1}^{N} \sum_{|\nu| \le q} \frac{1}{\nu!} D^\nu f(x_i)(x - x_i)^\nu \cdot W_i(x) \tag{B.3}$$

where $Q_i^q = \sum_{|\nu| \le q} \frac{1}{\nu!} D^\nu f(x_i)(x - x_i)^\nu$. The derivatives $D^\nu f(x_i)$ are computed based on finite difference method. As the first order direvatives of the velocities are needed in the Runge-Kutta method, here the Taylor series can also take first order direvatives, i.e. $q = 1$, without calculating higher order direvatives but achieving better precision than the original interpolation.

VITA

Bo Chen was born in Qianjiang, China. She finished her B.S. in electrical engineering at Wuhan University, 2007, and M.S. in electrical engineering at Texas A&M University, 2009. During her study in engineering, she had some opportunities to get in touch with geoscience and decided to pursue further education in this field. After her engineering study, she started her M.S. program in geophsycis with Dr. R. L. Gibson studying seismic wave propagation and imaging at Texas A&M University in 2009 and received her M.S. degree in geophysics in 2011. Her address is Department of Geology and Geophysics, 3115 TAMU, College Station, Texas, 77843-3115 and email address is bochen9@yahoo.com.

The typist for this thesis was Bo Chen.